



GLOBAL JOURNAL OF HUMAN-SOCIAL SCIENCE: G
LINGUISTICS & EDUCATION
Volume 22 Issue 5 Version 1.0 Year 2022
Type: Double Blind Peer Reviewed International Research Journal
Publisher: Global Journals
Online ISSN: 2249-460X & Print ISSN: 0975-587X

Several Slip Effects on MHD Flow of Casson Nanofluid Across a Porous Stretched Sheet in the Presence of Chemical Reactivity and Thermal Radiation

By K. Veera Reddy

Abstract- Multiple slip effects involving on the outflow of the boundary layer, first-order chemical processes, heat, radiation and mass Study examined into the transmission more stretching surface of a non-Newtonian nanofluid. To define liquid flow which is not Newtonian, the MHD Casson fluid approach is formulated. Through suitable the governing nonlinear Similarity transformations can be changed into an ODE system, might be numerically solved via 4th order Runge Kutta method as well as the shooting technique. Whenever a concentration slip parameter and a generative chemical reaction are used, the heat transfer rate increases, whereas when a chemical reaction that is harmful and a thermal slip parameter are used, the heat transfer rate drops. The numerical method is when comparison to earlier results in the literature, and there is a significant overlap.

GJHSS-G Classification: LCC Code: GB857.2.W2



Strictly as per the compliance and regulations of:



Several Slip Effects on MHD Flow of Casson Nanofluid Across a Porous Stretched Sheet in the Presence of Chemical Reactivity and Thermal Radiation

K. Veera Reddy

Abstract- Multiple slip effects involving on the outflow of the boundary layer, first-order chemical processes, heat, radiation and mass Study examined into the transmission more stretching surface of a non-Newtonian nanofluid. To define liquid flow which is not Newtonian, the MHD Casson fluid approach is formulated. Through suitable the governing nonlinear Similarity transformations can be changed into an ODE system, might be numerically solved via 4th order Runge Kutta method as well as the shooting technique. Whenever a concentration slip parameter and a generative chemical reaction are used, the heat transfer rate increases, whereas when a chemical reaction that is harmful and a thermal slip parameter are used, the heat transfer rate drops. The numerical method is when comparison to earlier results in the literature, and there is a significant overlap.

I. INTRODUCTION

Microelectronics, pharmaceutical processes, Fridge, heat transfer, Boiler flue gas temperature reduction, grinding, and machining all seems to be instances of engine cooling/vehicle thermal management.

Nadeem *et al.* [1] demonstrated an oblique Casson-nano fluid flow provided boundary conditions that seem to be convective. Nazari *et al.* [2] investigated propagation of entropy models for Casson nanofluid flow caused by a stretched surface. Haq *et al.* [3] Hari investigated the consequences of heat transmission and MHD on the Casson nanofluid across a shrinking sheet. Rashad [4] studied on the influence of unstable with a convective boundary condition, nano fluid flow across a leaning stretched surface. Within the presence of slip flow, Afify *et al.* [5] over a permeable stretched sheet, the MHD boundary layer flows, the effects of Newtonian heating on scaling group transformation were studied. El-Kabeir *et al.* [6] used a Casson fluid flows in a mixed convective flow around a sphere with partial slip, chemical reaction to demonstrate heat and mass transfer. Afify [7] studied heat transmission of nanofluids over an uneven stretched surface using slip flow and heat generation/absorption. Krishna *et al.* [8] Using a stretched porous sheet, they inquired the impact of chemical reactions on Casson fluid MHD flow. Nagasantoshi *et al.* [9] Nanofluid flow across with the

stretching sheet varying viscosity, non-uniform heat source was analyzed. Arundhati *et al.* [10] studied a nanofluid flow within a restricted wavy vertical channel with a flow of dual convective heat, mass transfer which is steadiness. Sivaiah *et al.* [11] in the radiation effect was explored numerically, the MHD Flow of the Boundary Layer model has been used to replicate the movement the transit of a viscoelastic and dissipative fluid thru a porous plate. About *et al.* [12] investigated the numerical assessment of natural disasters and global error estimates of convection effects on bacteria gliding over a porous non-Darcy substance on a power-law basis Slime consisting with nanoparticles. In the presence of a heat sink that is non uniform, Raju *et al.* [13] demonstrated non-Newtonian nanofluid over a cone, convective heat, mass transfer. Gayatri *et al.* [14] studied Carreau fluid over a stretched sheet, flow with viscous dissipation, Joule heating. Vijaya *et al.* [15] investigated a chemical reaction and viscous dissipation driven by a porous elongated sheet yields an electrically conducting Casson fluid flow. Choi [16] looked at using nanoparticles to produce fluids more thermally conductive. Lee *et al.* [17] Thermal conductivity were explored of the fluids using oxide nanoparticles. Many researchers [18-29] have since researched at the wall, there is a velocity fall and a temperature jump with nanofluid and viscous fluids using various geometries.

The purpose of paper is to investigate the boundary conditions on thermal, concentration slip fluid flow, velocity, and chemical reaction in Casson, heat transfer stretching with nanoparticles on the surface because of Brownian diffusion and thermophoresis in Casson, heat transfer over a stretching. The velocity, temperature, and nanoparticle concentration fields' numerical results are presented. The friction as the heat and mass transfer rates, tabulated and assessed. The nanoparticles imbedded in Casson fluid have a number of practical applications, according to the current study, including nuclear reactors, microelectronics, and chemical production.

II. FORMULATION OF MATHEMATICS

Consider the MHD an inexhaustible Casson nanofluids past a porous stretching surface with a steady boundary layer. The sheet has been stretched at the linear velocity. The x-axis behaves similarly to the

continuous stretching porous sheet, while the y-direction flows transverses. It is considered that the flow proceeds for a period of time. At the surface, temperature and concentration fixed at exact constant

values, T , C are fixed values which are fixed a long way below the surface a 1st order homogeneous chemical reaction of species with a reaction rate constant, K_l , is also assumed. Fig.1 shows a flow diagram.

The rheological equation, for state a Casson fluid flow that also isotropic and incompressible is given by Ramana Reddy et al. [29]:

$$\tau_{ij} = \begin{cases} 2\left(\mu_B + \frac{P_y}{\sqrt{2\pi}}\right)e_{ij}, & \pi > \pi_c \\ 2\left(\mu_B + \frac{P}{\sqrt{2\pi_c}}\right)e_{ij}, & \pi < \pi_c \end{cases} \quad (1)$$

where μ_B is the non-Newtonian fluid plastic dynamic viscosity, P_y - the yield stress, π - the product of the component of deformation rate and itself, precisely, $\pi = e_{ij}e_{ij}$, e_{ij} = the (i,j)th component of the deformation rate, and c is a critical value of based on non-Newtonian model.

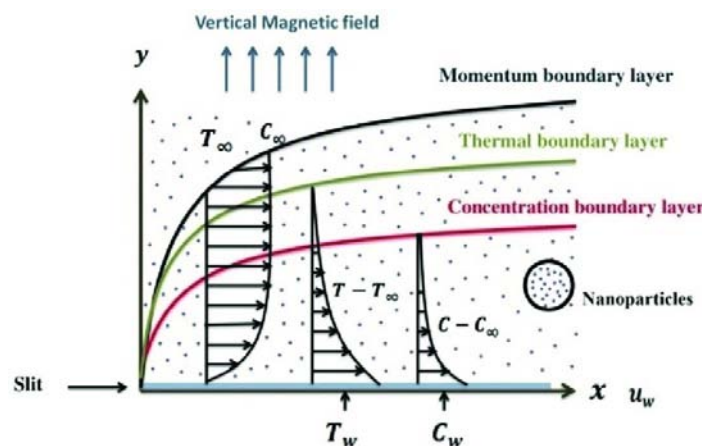


Figure 1: The Physical model and coordinate system.

The governing equations of Casson nanofluid can be expressed with boundary layer approximations:

$$\frac{\partial u}{\partial x} + \frac{\partial v}{\partial y} = 0 \quad (2)$$

$$u \frac{\partial u}{\partial x} + v \frac{\partial v}{\partial y} = \nu \left(1 + \frac{1}{\beta} \right) \frac{\partial^2 u}{\partial x^2} - \left(\frac{\nu}{k} u + \frac{\sigma B_0^2}{\rho} u \right) \quad (3)$$

$$u \frac{\partial T}{\partial x} + v \frac{\partial T}{\partial y} = \alpha \frac{\partial^2 T}{\partial y^2} + \tau \left\{ D_B \left(\frac{\partial C}{\partial y} \frac{\partial T}{\partial y} \right) + \frac{D_T}{T_\infty} \left(\frac{\partial T}{\partial y} \right)^2 \right\} + \left(1 + \frac{1}{\beta} \right) \frac{\mu}{\rho C_p} \left(\frac{\partial u}{\partial y} \right)^2 - \frac{1}{\rho C_p} \frac{\partial q_r}{\partial y} \quad (4)$$

$$u \frac{\partial C}{\partial x} + v \frac{\partial C}{\partial y} = \alpha \frac{\partial^2 C}{\partial y^2} + D_B \frac{\partial^2 C}{\partial y^2} + \frac{D_T}{T_\infty} \frac{\partial^2 T}{\partial y^2} - K_l (C - C_\infty) \quad (5)$$

The boundary conditions

$$u = u_w + \left(1 + \frac{1}{\beta} \right) N \rho \nu \frac{\partial u}{\partial y}, \quad v = 0, \quad T = T_w + K_1 \frac{\partial T}{\partial y} \quad \text{at } y = 0 \quad (6)$$

$$u = 0, \quad T = T_\infty, \quad C = C_\infty \quad \text{as } y \rightarrow \infty$$

where u and v are velocity components with the x - and y -axes respectively, ρ is the fluid density, ν is the fluid

kinematic viscosity, $\alpha = \frac{k}{pCp}$ is the fluid's thermal diffusivity, $\tau = \frac{(\rho C)_p}{(\rho C)_f}$ - the ratio between the nanoparticles and the heat capacity of fluids, q_r is radiative heat flux, D_B - the Brownian diffusion coefficient, and D_T is the thermophoretic diffusion coefficient. Furthermore, N , K_1 , and K_2 are velocity, thermal, and concentration slip factor. In order to simplify the radiative heat flux on the flow, we have given the preference to the application of Roseland diffusion approximation as follows:

In view of equations (7) and (8), equation (4) reduces to

$$u \frac{\partial T}{\partial x} + v \frac{\partial T}{\partial y} = \alpha \frac{\partial^2 T}{\partial y^2} + \tau \left\{ D_B \left(\frac{\partial C}{\partial y} \frac{\partial T}{\partial y} \right) + \frac{D_T}{T_\infty} \left(\frac{\partial T}{\partial y} \right)^2 \right\} + \left(1 + \frac{1}{\beta} \right) \frac{\mu}{\rho C_p} \left(\frac{\partial u}{\partial y} \right)^2 + \frac{16\sigma_s T_\infty^3}{3\rho c_p k_e} \frac{\partial^2 T}{\partial y^2} \quad (9)$$

The non-dimensional variables enumerated are expressed as follows:

$$\eta = y \sqrt{b/v}, \quad \psi(x, y) = x \sqrt{bv} f(\eta), \quad \theta(\eta) = \frac{T - T_\infty}{T_w - T_\infty},$$

$$\varphi(\eta) = \frac{C - C_\infty}{C_w - C_\infty}, \quad M = \frac{\sigma B_0^2 \nu}{\rho v_0^2}, \quad K = \frac{K' v_0^2}{\nu^2}, \quad R = \frac{16\sigma^* T_\infty^3}{3K_s} \quad (10)$$

The stream function (x, y) is provided to obey the equation continuity (2).

$$u = \frac{\partial \psi}{\partial y}, \quad v = -\frac{\partial \psi}{\partial x} \quad (11)$$

As a function of the above modifications (3), (5), (9), are reduced to

$$\left(1 + \frac{1}{\beta} \right) f''' + ff'' - f'^2 + \left(M + \frac{1}{K} \right) f' = 0 \quad (12)$$

$$\left(\frac{1+R}{P_r} \right) \theta'' + \theta' f + Nb\theta'\varphi' + Nt\theta'^2 + E_c \left(1 + \frac{1}{\beta} \right) f''^2 = 0 \quad (13)$$

$$\varphi'' + Le f \varphi' + \frac{Nt}{Nb} \theta'' - Le Kr\varphi = 0 \quad (14)$$

boundary circumstances are:

$$f(0) = 0, f'(0) = 1 + L_1 \left(1 + \frac{1}{\beta} \right) f''(0), \quad \theta(0) = 1 + L_2 \theta'(0), \quad \varphi(0) = 1 + L_3 \varphi'(0) \quad (15)$$

$$f'(\infty) = 0, \theta(\infty) = 0, \varphi(\infty) = 0$$

$$q_r = -\frac{4\sigma_s^*}{3k_e^*} \frac{\partial T^4}{\partial y} \quad (7)$$

where σ_s^* = Stefan-Boltzman constant and k_e^* = the mean absorption coefficient. The study is focused to thin fluids owing to the Roseland approximation. eqn (7) can be mathematically expressed if the temperature differential within the flow is tiny indeed by extending T^4 using Taylors series about T_∞ and neglecting higher order terms, we obtain

$$T^4 = 4T_\infty^3 T - 3T_\infty^4 \quad (8)$$

Differentiation with respect η is expressed by the term prime, f is function of similarity, θ is the temperature that has dimensionless, ϕ is the volume percentage of dimensionless nanoparticles, $P_r = \nu/\alpha$ is Prandtl number, $L_e = \nu/D_B$ is Lewis number, $\gamma = K_1 \sqrt{(b/\nu)}$ is the thermal slip parameter, $\beta = \mu_B \sqrt{2\pi_c}/P_y$ is the Casson parameter, $\lambda = Np\sqrt{(vb)}$ is the slip parameter, $\delta = K_2(b/\nu)^{1/2}$ is the concentration slip parameter, $E_c = u_w^2/C_p(T_w - T_\infty)$ is the Eckert number, $Kr = K_0/b$ is the chemical reaction parameter, $Nb = (\rho C)_p D_B (C_w - C_\infty)/(\rho C)_f \nu$ is the Brownian motion parameter, and $Nt = (\rho C)_p D_T (T_w - T_\infty)/(\rho C)_f \nu T_\infty$ is the thermophoresis parameter, respectively. The quantities of physical interest in this problem are the local skin friction coefficient C_{fx} , the local Nusselt number Nu_x , and local Sherwood number Sh_x , Magnetic field parameter M, Radiation parameter R, permeability parameter K, which are defined as

$$C_{fx} = \frac{\tau_w}{\rho u_w^2}, \quad Nu_x = \frac{xq_w}{K(T_w - T_\infty)}, \quad Sh_x = \frac{xq_m}{D_B(C_w - C_\infty)} \quad (16)$$

where τ_w is the shear stress, q_w and q_m are the surface heat and mass flux which are given by the following expressions:

$$\tau_w = \left(\mu_B + \frac{P_y}{\sqrt{2\pi_c}} \right) \left(\frac{\partial u}{\partial y} \right)_{y=0}, \quad q_w = -K \left(\frac{\partial T}{\partial y} \right)_{y=0}, \quad q_m = -D_B \left(\frac{\partial C}{\partial y} \right)_{y=0} \quad (17)$$

The dimensionless forms of skin friction, the local Nusselt number, and the local sherwood number become

$$\sqrt{Re_x} C_f = \left(1 + \frac{1}{\beta} \right) f''(0), \quad \frac{Nu_x}{\sqrt{Re_x}} = -\theta'(0), \quad \frac{Sh_x}{\sqrt{Re_x}} = -\varphi'(0)$$

where $Re_x = xu_w/\nu$ is the local Reynolds number.

a) Numerical Solution

The dimensionless equations are the beginning and boundary conditions, were numerically solved using the 4th order R-K method and the shooting approach. By assigning various numerical values to the dimensionless governing parameters, the effect of dimensionless governing variables on velocity, temperature, and concentration fields, skin friction

number, $Kr = K_0/b$ is the chemical reaction parameter, $Nb = (\rho C)_p D_B (C_w - C_\infty)/(\rho C)_f \nu$ is the Brownian motion parameter, and $Nt = (\rho C)_p D_T (T_w - T_\infty)/(\rho C)_f \nu T_\infty$ is the thermophoresis parameter, respectively. The quantities of physical interest in this problem are the local skin friction coefficient C_{fx} , the local Nusselt number Nu_x , and local Sherwood number Sh_x , Magnetic field parameter M, Radiation parameter R, permeability parameter K, which are defined as

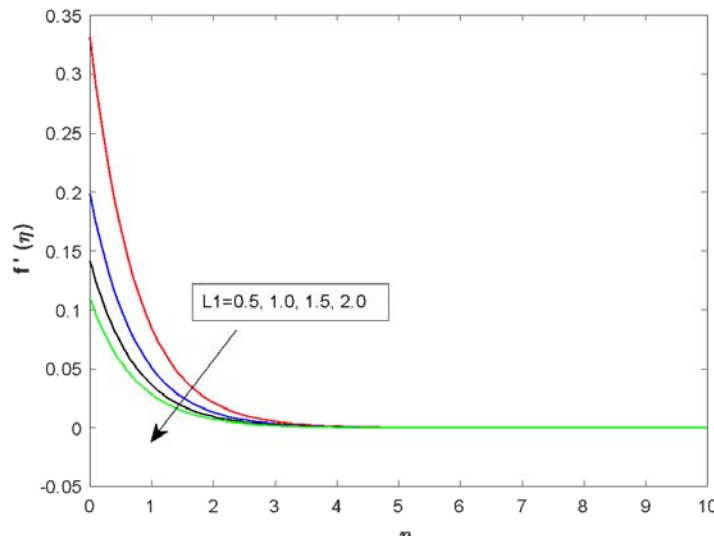


Fig. 2: Velocity profiles

factor, Nusselt number, and shearwood number has been shown. The outcomes are reviewed and presented in the form of tables and graphs. Dimensionless governing parameters include the flow slip variable (L1), the thermal slip parameter (L2), the concentration slip parameter (L3), the magnetic (M), the Casson fluid (β)

Fig.2 represents the velocity profiles for various values of flow slip parameter. It has been noticed that as the slip parameter increases, velocity decreases. Because of the slip parameter, resistance pressure is

produced adjacent to the stretching porous sheet, lowering the Friction factor, heat transfer rate, and mass transfer rate are all factors to consider.

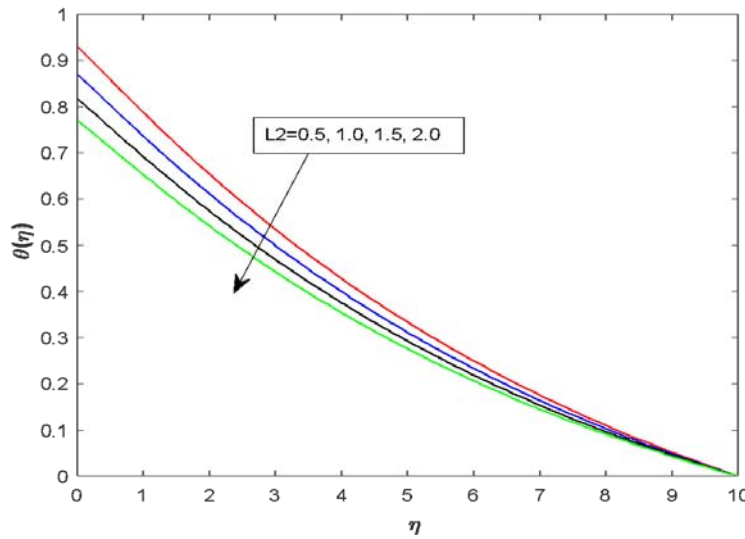


Fig. 3: Temperature plot

Fig. 3 depicts the effect of thermal slip parameter on the temperature plot. The temperature drops as the thermal slip parameter (L_2) grows, as

shown in the figure. As the thermal slip parameter is raised, the heat transfer rate falls.

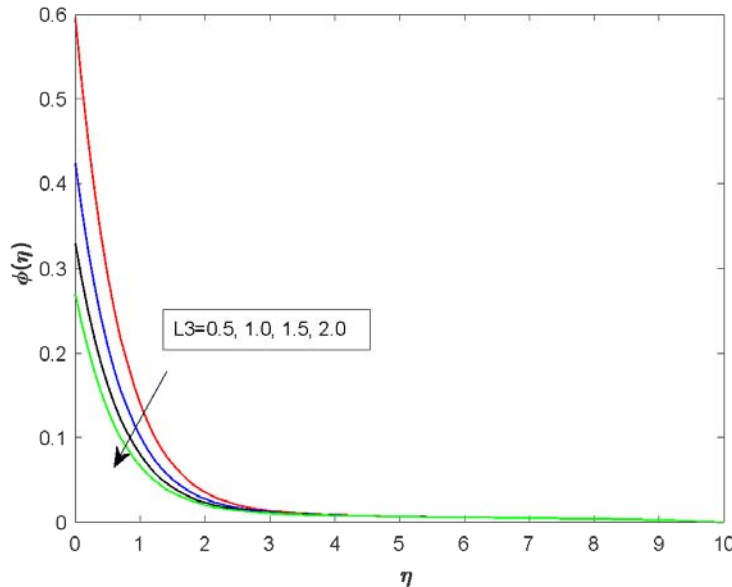


Fig. 4: Concentration profiles

The effect of concentration slip parameter (L_3) on the concentration profiles is shown in Fig.4. It is observed that the slip parameter increases, the concentration distribution decreases. The mass transfer rate reduces as a consequence.



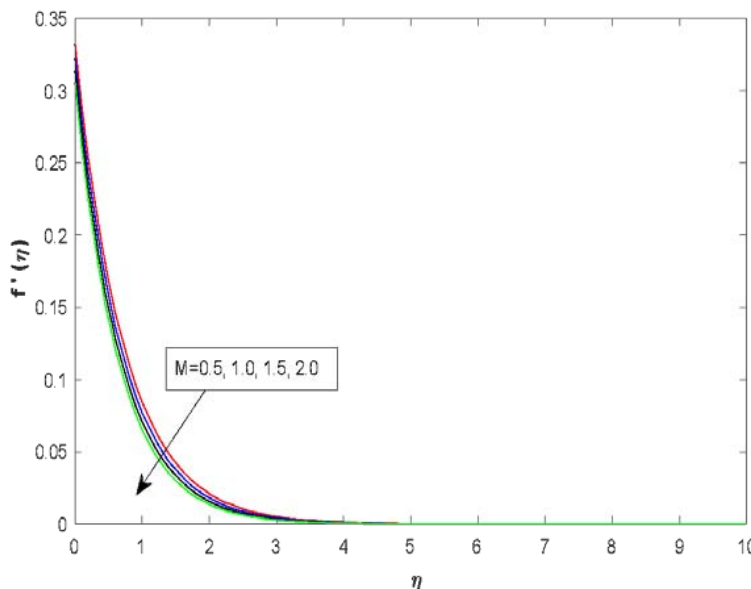


Fig. 5: Velocity profile

Fig. 5 presents the outcomes of external magnetic field (M) on the velocity profile. It should be emphasized that as M grows, the fluid velocity reduces. This is owing to the presence of a transverse magnetic

field, which causes a sudden drag force (Lorenz force) opposing the Casson fluid's motion and so delays the flow velocity.

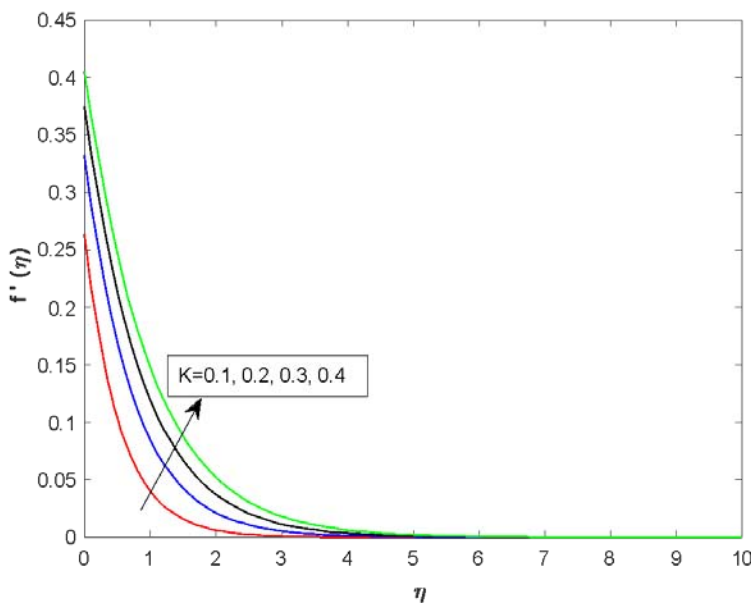


Fig. 6: Velocity profiles

The impact of the permeability plot on dimensionless velocity is shown in Fig. 6. It is worth noting that an increase in porous medium, the results of the fluid velocity increases.

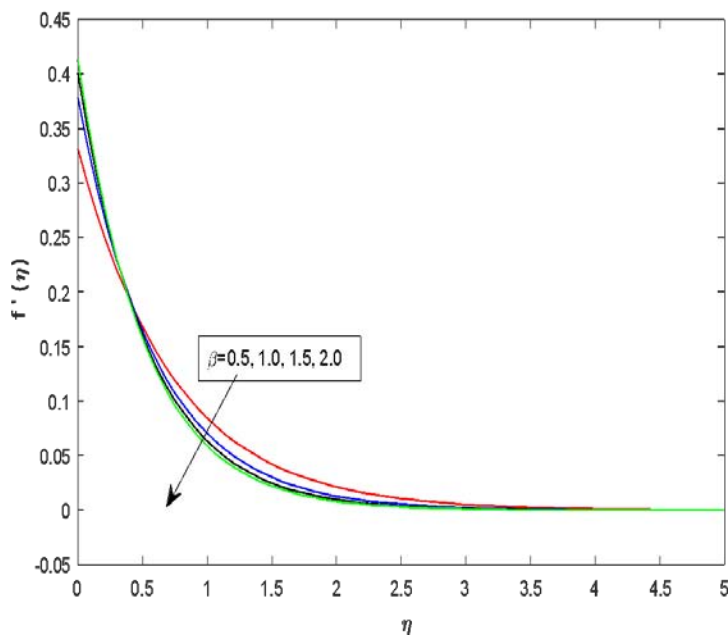


Fig. 7: Velocity profiles

The effect of Casson fluid plot on dimensionless velocity is shown in Fig. 7 and observed that the velocity decreases with an increase of Casson fluid parameter $0.5 \leq \beta \leq 3.0$. It is necessary because the lowering of the yield stress of the Casson fluid decreases. Physically,

an increase in the Casson parameter to minimize the yield stress which means that plastic dynamic viscosity of the fluid is increased and that the momentum boundary layer becomes thicker.

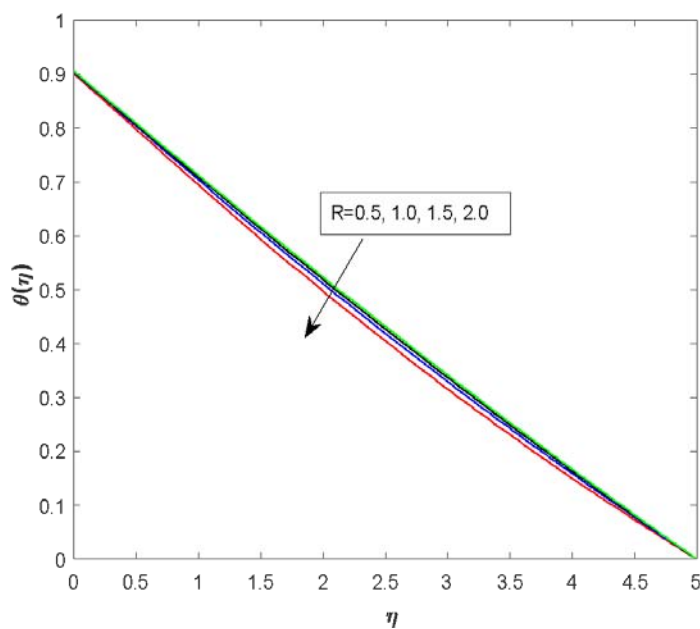


Fig. 8: Temperature profiles

Fig. 8 shows the effect of radiation parameter on the temperature profiles. When the radiation parameter is enhanced, the temperature decreases. This is owing to the thinness of the temperature boundary layer.

Table 1: Comparison table $\left(1 + \frac{1}{\beta}\right) f''(0), -\theta'(0), -\phi'(0)$ different values of $L1, L2, L3, \beta$

L1	L2	L3	β	$\left(1 + \frac{1}{\beta}\right) f''(0)$ Afify	$\left(1 + \frac{1}{\beta}\right) f''(0)$ Present	$-\theta'(0)$ Afify	$-\theta'(0)$ present	$-\phi'(0)$ Afify	$-\phi'(0)$ Present
0	0.2	0.2	0.5	-1.733100	-1.733105	0.628232	0.628235	1.324400	1.324412
1	0.2	0.2	0.5	-0.541057	-0.541053	0.587859	0.587857	1.047300	1.047350
3	0.2	0.2	0.5	-0.243961	-0.243963	0.473596	0.473590	0.972528	0.972530
0.2	0	0.2	0.5	-1.164996	-1.164999	0.763040	0.763042	1.172730	1.172735
0.2	1	0.2	0.5	-1.164996	-1.164998	0.411102	0.411108	1.241970	1.241972
0.2	3	0.2	0.5	-1.164996	-1.164998	0.208327	0.208329	1.288470	1.288476
0.2	0.2	0	0.5	-1.164996	-1.164997	0.620139	0.620142	1.639360	1.639362
0.2	0.2	1	0.5	-1.164996	-1.164998	0.707216	0.707220	0.569352	0.569354
0.2	0.2	3	0.5	-1.164996	-1.164999	0.734532	0.734538	0.246761	0.246762
0.2	0.2	0.2	0.3	-1.319520	-1.319525	0.651801	0.651808	1.188420	1.188421
0.2	0.2	0.2	4	-0.846526	-0.86530	0.655087	0.655082	1.185290	1.185292
0.2	0.2	0.2	∞	-0.776388	-0.776385	0.652042	0.652048	1.179710	1.179713

III. CONCLUSIONS

The following are the key findings of this study:

1. As the slip variable increases, the velocity reduces.
2. The temperature drops as the thermal slip plot is increased.
3. The concentration distribution shrinks as the slip parameter grows.
4. As the magnetic parameter increases, the fluid velocity decreases.
5. As the Casson fluid parameter is increased, the velocity falls.

REFERENCES RÉFÉRENCES REFERENCIAS

1. Nadeem. S, Mehmood. R, and Akbar. N. S, "Optimized analytical solution for oblique flow of a Casson-nano fluid with convective boundary conditions," International Journal of Thermal Sciences, vol. 78, pp. 90–100, 2014.
2. Abolbashari. M.H, Freidoonimehr. N, Nazari. F, and Rashidi. M, "Analytical modeling of entropy generation for Casson nano-fluid flow induced by a

stretching surface," Advanced Powder Technology, vol. 26, no. 2, pp. 542–552, 2015.

3. Haq. R. U, Nadeem. S, Khan. H. Z, and Okedayo. T. G, "Convective heat transfer and MHD effects on Casson nanofluid flow over a shrinking sheet," Central European Journal of Physics, vol. 12, no. 12, pp. 862–871, 2014.
4. A. Rashad, "Unsteady nanofluid flow over an inclined stretching surface with convective boundary condition and anisotropic slip impact," International Journal of Heat and Technology, vol. 35, no. 1, pp. 82–90, 2017.
5. A. A. Afify, M. J. Uddin, and M. Ferdows, "Scaling group transformation for MHD boundary layer flow over permeable stretching sheet in presence of slip flow with Newtonian heating effects," Applied Mathematics and Mechanics, vol. 35, no. 11, pp. 1375–1386, 2014.
6. S. M. M. El-Kabeir, E. R. El-Zahar, and A. M. Rashad, "Effect of chemical reaction on heat and mass transfer by mixed convection flow of casson fluid about a sphere with partial slip," Journal of

Computational and Theoretical Nanoscience, vol. 13, no. 8, pp. 5218–5226, 2016.

7. A. A. Afify, "Slip effects on the flow and heat transfer of nanofuids over an unsteady stretching surface with heat generation/absorption," Journal of Computational and Theoretical Nano science, vol. 12, no. 3, pp. 484–491, 2015.
8. Krishna Y.H., Reddy G.V.R., Makinde O.D.(2018), 'Chemical reaction effect on MHD flow of casson fluid with porous stretching sheet', Defect and Diffusion Forum ,389, PP. 100-109.
9. Nagasantosh P., Ramana Reddy G.V., Gnaneswara Reddy M., Padma P.(2018), 'Nanofuid flow over a stretching sheet with non-uniform heat source and variable viscosity', Journal of Nanofuids ,7(5), PP. 821-832
10. Arundhati V., Chandra Sekhar K.V., Prasada Rao D.R.V., Sreedevi G. (2019), 'Unsteady mixed convective heat and mass transfer flow of nanofuid in a constricted vertical wavy channel', JP Journal of Heat and Mass Transfer, 18(1), PP. 35-56.
11. Sivaiah G., Jayarami Reddy K., Chandra Reddy P., Raju M.C. (2019), 'Numerical study of mhd boundary layer flow of a viscoelastic and dissipative fluid past a porous plate in the presence of thermal radiation', International Journal of Fluid Mechanics Research, 46(1), PP.27-38.
12. M. Y. Abou-Zeid, A. A. Shaaban, and M. Y. Alhour, "Numerical treatment and global error estimation of natural convective effects on gliding motion of bacteria on a power-lawnanoslime through a non-darcy porous medium," Journal of Porous Media, vol. 18, no. 11, pp. 1091–1106, 2015.
13. A. S. K. Raju, N. Sandeep, and A. Malvandi, "Free convective heat and mass transfer of MHD non-Newtonian nanofuids over a cone in the presence of non-uniform heat source/sink," Journal of Molecular Liquids, vol. 221, pp. 108–115, 2016.
14. Gayatri, M., Reddy, K. J., Babu, M. J. Slip flow of Carreau fluid over a slendering stretching sheet with viscous dissipation and Joule heating, *SN Applied Sciences*, 2(3), 2020, 1-11.
15. Vijaya, N., Arifuzzaman, S. M., Raghavendra Sai, N., Rao, M. Analysis of Arrhenius activation energy in electrically conducting casson fluid flow induced due to permeable elongated sheet with chemical reaction and viscous dissipation, *Frontiers in Heat and Mass Transfer (FHMT)*, 15(1), 2020.
16. S. U. S. Choi, "Enhancing thermal conductivity of fluids with nanoparticles," in Proceedings of the in Proceedings of the 1995 ASME International Mechanical Engineering Congress and Exposition, vol. 66, pp. 99–105, San Francisco, Calif, USA, 1995.
17. S. Lee, S. U. Choi, S. Li, and J. A. Eastman, "Measuring thermal conductivity of fluids containing oxide nanoparticles," *Journal of Heat Transfer*, vol. 121, no. 2, pp. 280–289, 1999.
18. Gladys T., G.V. Ramana Reddy (2022) Contributions of variable viscosity and thermal conductivity on the dynamics of non-Newtonian nanofuids flow past an accelerating vertical plate. *Partial Differential Equations in Applied Mathematics* 5 (2022) 100264. Doi: <https://doi.org/10.1016/j.padiff.2022.100264>.
19. M. K. Nayak, G. Mahanta, K. Karmakar, P. Mohanty, S. Shaw (2022) Effects of Thermal Radiation and Stability Analysis on MHD Stagnation Casson Fluid Flow Over the Stretching Surface with Slip Velocity. *AIP Conference Proceedings* 2435, 020045 (2022); Doi: <https://doi.org/10.1063/5.0084385>.
20. Elham Alali and Ahmed M. Megahed (2022) MHD dissipative Casson nanofuid liquid film flow due to an unsteady stretching sheet with radiation influence and slip velocity phenomenon. *Nanotechnology Reviews* 2022; 11: 463–472 <https://doi.org/10.1515/ntrev-2022-0031>
21. Seethamahalskshmi, G. V. Ramana Reddy, A. Sandhya, D. Sateesh Kumar (2021) Study MHD mixed convective flow of a vertical porous surface in the presence viscous dissipation. *AIP Conference Proceedings* 2375, 030009 (2021); Doi: <https://doi.org/10.1063/5.0066915>.
22. V Malapati, DV Lakshmi (2021) Diffusion-thermo and heat source effects on the unsteady radiative MHD boundary layer slip flow past an infinite vertical porous plate. *Journal of Naval Architecture and Marine Engineering* 18 (1), 55-72, DOI: <https://doi.org/10.3329/jname.v18i1.33024>.
23. P. Suresh, Y. Hari Krishna, S. Hari Singh Naik, P. V. Janardhana Reddy (2021) Heat and Mass Transfer in MHD Casson Fluid Flow along Exponentially Permeable Stretching Sheet in Presence of Radiation and Chemical Reaction. *Annals of R.S.C.B.*, ISSN: 1583-6258, Vol. 25, Issue 1, 2021, Pages. 7163-7175. Doi: <http://annalsofrscb.ro>.
24. Karnati Veera Reddy, Gurrampati Venkata Ramana Reddy (2022). Outlining the Impact of Melting on Mhd Casson Fluid Flow Past a Stretching Sheet in a Porous Medium with Radiation. *Biointerface Research in Applied Chemistry*, 13, (1), 2023, 42.
25. Vishalakshi, A.B. Mahabaleshwar, U.S.; Sarris, I.E. An MHD Fluid Flow over a Porous Stretching/ Shrinking Sheet with Slips and Mass Transpiration. *Micromachines* 2022, 13, 116. Doi: <https://doi.org/10.3390/mi13010116>.
26. Eleni Seid, Eshetu Haile, Tadesse Waleign. Multiple slip, Soret and Dufour effects in fluid flow near a vertical stretching sheet in the presence of magnetic nanoparticles. *International Journal of Thermofluids* 13 (2022) 100136. Doi: <https://doi.org/10.1016/j.ijft.2022.100136>.



27. Reddy KV, Ramana Reddy GV, Sandhya A, Krishna YH. Numerical solution of MHD, Soret, Dufour, and thermal radiation contributions on unsteady free convection motion of casson liquid past a semi-infinite vertical porous plate. *Heat Transfer*. 2022; 1-22. doi:10.1002/htj.22452.
28. Ahmed A, Afify, The Influence of Slip Boundary Condition on Casson Nanofuid Flow over a Stretching Sheet in the Presence of Viscous Dissipation and Chemical Reaction. *Journal of Mathematical Problems in Engineering*. 2017, Article ID 3804751. doi: <https://doi.org/10.1155/2017/3804751>
29. Reddy KV, Reddy GVR, Krishna Yaragani H. Effects of Cattaneo–Christov heat flux analysis on heat and mass transport of Casson nanoliquid past an accelerating penetrable plate with thermal radiation and Soret–Dufour mechanism. *Heat Transfer*. 2020; 1–22. <https://doi.org/10.1002/htj.22036>.